Geometry of Porous Hydroxyapatite Implants Influences Osteogenesis in Baboons (*Papio ursinus*)

Ansuyah Magan, BSc, BDS, MSc
Ugo Ripamonti, MD, PhD
Johannesburg, South Africa

Coral-derived porous hydroxyapatite disks of two geometric configurations were implanted in 16 calvarial defects, 25 mm in diameter, prepared in eight subadult male baboons (*Papio ursinus*). To determine whether the orientation of the exoskeletal microstructures (corallites) influences bone ingrowth and osteogenesis, hydroxyapatite disks were prepared by cutting the coral either longitudinally or transversally, to obtain two distinct implant geometries defined by the orientation of the corallites. In the same animals, 16 defects were left untreated to assess the regeneration potential of the subadult baboon calvaria. Disks of both geometric configurations were also implanted in heterotopic intramuscular sites to investigate their osteoinductive potential. Histomorphometric analysis on undecalcified and decalcified sections prepared from specimens harvested on day 90 after surgery showed that greater amounts of bone formed in porous hydroxyapatites cut in the longitudinal plane when compared with hydroxyapatites cut in the transversal plane ($p < 0.01$). Bone formed in hydroxyapatite specimens harvested from the intramuscular sites, but no difference in bone formation was found between the two geometric configurations. Untreated defects showed limited osteogenesis, comparable with a previous series of untreated defects identically prepared in adult baboon calvariae. This finding suggests that skeletally mature, adult primates may not be a requirement for evaluation of craniofacial bone substitutes. These results in a primate indicate that hydroxyapatite disks are able to induce bone differentiation when implanted in intramuscular sites, and that the geometric configuration of the porous hydroxyapatite influences bone ingrowth and osteogenesis in orthotopic calvarial sites. This should be taken into consideration when designing porous bone substitutes for craniofacial applications.

Key Words: Primates, calvarial defects, porous hydroxyapatite, implant geometry, osteogenesis, bone morphogenetic proteins

Incorporation and long-term stability of craniofacial porous bone substitutes is dependent on bone ingrowth from surrounding viable bone. To limit the harvesting of autogenous bone grafts and associated complications, sintered and coral-derived porous hydroxyapatites have been investigated extensively as bone substitutes [1, 2], solo or in combination with bone morphogenetic proteins (BMPs), which initiate local bone formation by induction in vivo ([3] for review). In spite of technologic advances in implant design and fabrication, bone growth into porous hydroxyapatites may not occur along the entire implant when evaluated on histologic criteria [4]. Excluding failures attributable to improper hydroxyapatite design, implant micromotion, and infection, lack of optimal osteoconductivity and osteointegration may be due to inadequate biologic consideration of the geometric configuration of the implant.

In a series of experiments in primates, we have shown that a specific configuration of a porous hydroxyapatite, obtained after hydrothermal conversion of the calcium carbonate exoskeleton of corals, is capable of inducing bone differentiation when implanted intramuscularly in adult baboons [5, 6]. It is noteworthy that in these experiments in heterotopic sites of the baboon, bone was found in porous hydroxyapatite only in block configuration. On the contrary, bone did not form in identical hydroxyapatite in granular configuration [7]. This underscores the importance of the geometry of the substratum as reported in early experiments in rodents showing lack of bone differentiation in granular hydroxyapatite even if pretreated with BMPs [8].

From the Bone Research Laboratory of the Medical Research Council and the University of the Witwatersrand, Johannesburg, and the Department of General Anatomy, University of the Witwatersrand, Johannesburg, South Africa.

Address correspondence to Dr Ripamonti, Bone Research Laboratory, MRC/University of the Witwatersrand, Medical School, 7 York Road, Parktown 2193 Johannesburg, South Africa.

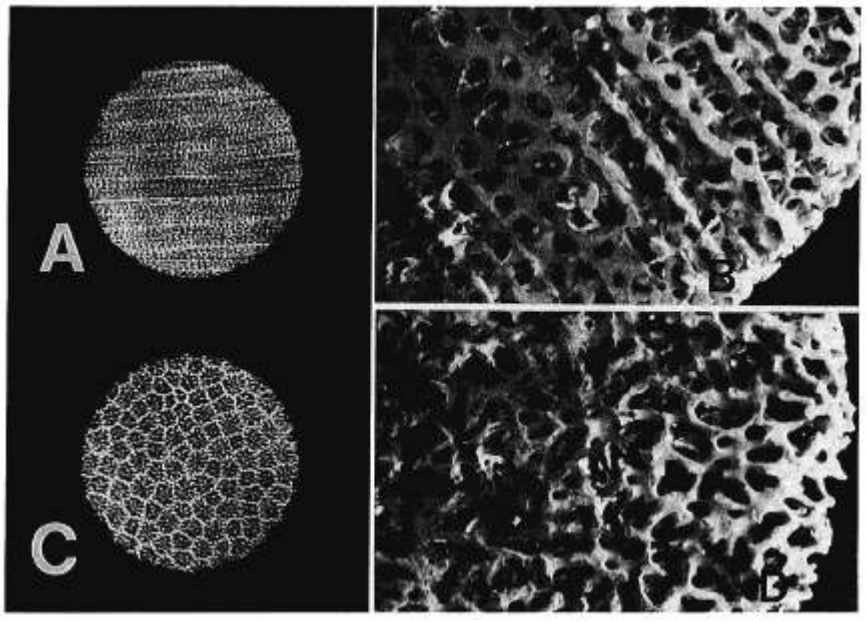

Fig 1 Physical characteristics of porous hydroxyapatite disks before implantation. (A and B) Radiograph and scanning electron images of a disk in which the original coral structure was cut in the longitudinal plane, along the scleroseptal channels of the corallites. (C and D) Disk cut in the transversal plane, showing the "rosette-like" pattern formed by individual corallites. Note interconnectivity of porous spaces in both geometric configurations.

Thus, it is likely that the geometric configuration of the porous hydroxyapatite may also influence the extent of bone formation when implanted in orthotopic craniofacial sites, in close proximity to viable bone. Implantation of porous hydroxyapatite in calvarial defects of adult dogs and baboons has occasionally resulted in fibrous union at the hydroxyapatite-calvarial interface, in spite of extensive bone deposition within the implant [4, 9]. In this study, using the primate calvarial model, we have investigated the influence of orientation of the exoskeletal microstructure of porous hydroxyapatite on bone ingrowth and osteogenesis. Porous hydroxyapatites with different geometric configurations were also implanted in heterotopic sites to investigate their osteoinductive potential. In the present experiments, subadult, instead of adult and skeletally mature baboons, were used as recipients. Although it has been suggested that younger animals retain a superior bone repair potential, no data were available on nonhuman primates regarding the incorporation of any kind of bone substitute in subadult versus adult individuals.

In this article, we report that the geometric configuration of the porous hydroxyapatite influences osteogenesis in orthotopic calvarial sites, and that the extent of bone regeneration in untreated calvarial defects of subadult baboons does not differ significantly when compared with adult baboons.

Materials and Methods

Primates

Eight clinically healthy subadult male Chacma baboons (*Papio ursinus*), with a mean weight of 25.2 kg, were selected from the primate colony at this University. Housing conditions and diet were as described previously [10]. Subadult baboons still have epiphyseal growth plates, as judged by radiographic examination of the distal epiphysis of the radius and ulna, but almost complete eruption of the large canines has occurred [11]. Research protocols were approved by the Animal Ethics Screening Committee of the University. Experimental procedures were conducted according to the *Guidelines for the Use and Care of Animals* of the University of the Witwatersrand, Johannesburg.

Hydroxyapatite Implants

Porous hydroxyapatites were prepared by Interpore International (Irvine, CA). Implants consisted of disks of porous hydroxyapatite obtained after hydrothermal conversion of the calcium carbonate exoskeleton of the coral Goniopora [12] into an inorganic replica of hydroxyapatite [13–15]. Each disk represents a collection of corallites, that is, exoskeletons of individual polyps. Each corallite consists of a thin basal plate from which fenestrated partitions, or scleroseptae, radiate vertically, dividing the original lumen occupied by the polyp's mesentery into 12 sections [12]. In Goniopora, the scleroseptal channels have an average diameter of 600 μm, whereas that of the fenestrated interconnections averages 260 μm. The average width of the solid components of the framework and their interconnections are 130 and 220 μm, respectively [15]. When cut in a longitudinal plane in relation to the corallites, a pattern of longitudinally running channels is seen on the surface of the hydroxyapatite disk; but when the corallites are cut transversally, a "rosette-like" pattern occurs as a result of the radiating septae (Fig 1). Disks used in this study were cut in the longitudinal and transversal planes and measured 25 mm in diameter, with a minimal

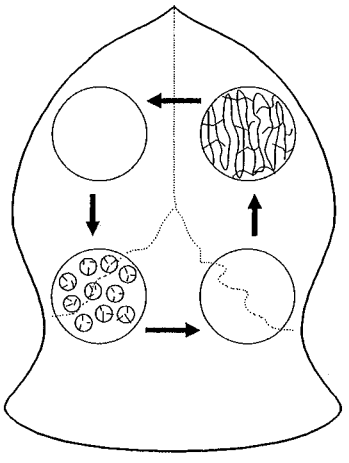

Fig 2 Calvarial model and implantation design in eight subadult male baboons. The Latin block design resulted in the rotational allocation of the three treatment methods within a total of 32 defects. Note the contralateral insertion of hydroxyapatite implants cut in the longitudinal and transversal planes. *Arrows* indicate the anticlockwise treatment rotation.

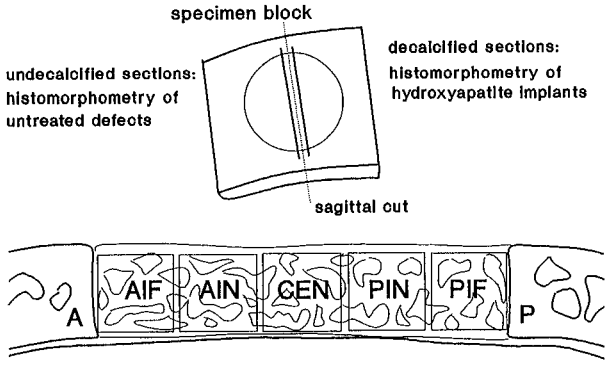

Fig 3 (Top) Histological processing for preparation of undecalcified and decalcified serial sections for histologic and histomorphometric analyses. (Bottom) Schematic calvarial section showing the five sources selected for histomorphometry. Sources, defined as the regions on which quantitative morphometry was performed [19], were anterior and posterior interfacial regions (AIF and PIF), anterior and posterior internal regions (AIN and PIN), and a central region (CEN). A and P indicate the anterior and posterior recipient calvarial margins.

thickness of 3.5 mm at the center. The endocranial aspect of the disks was prepared with either a planar or a spherical concave surface in relation to the site of implantation, thus conforming to the curvature of the baboon calvaria [9].

Surgical Procedures and Experimental Design

On the evening before surgery, food was withdrawn but animals had access to water ad libitum. On the day of surgery, the baboons were immobilized with intramuscular injections of ketamine hydrochloride (10 mg/kg). Anesthesia was induced by intravenous sodium thiopentone (15 mg/kg) and maintained with halothane vapor in 100% oxygen after orotracheal intubation. Ringer's lactate (600 ml) was administered intravenously to each animal for the duration of surgery.

Orthotopic Calvarial Implantation

The development of the primate calvarial model to test the osteogenic potential of different bone substitutes has been described in detail [9, 16, 17]. On each side of the calvaria, two full-thickness defects, 25 mm in diameter, were prepared with a craniotome. In each animal, one defect was implanted with a disk of hydroxyapatite cut in the transversal plane and a second defect implanted with a disk of hydroxyapatite cut in the longitudinal plane. The remaining two defects were left untreated to evaluate the regeneration potential of the subadult baboon calvaria. A Latin block design was used to allocate the position of the implants and the untreated defects [9, 16] (Fig 2). Disks were inserted by friction-fit into the defects and no additional fixation was performed. Hydroxyapatite disks cut in the longitudinal plane were inserted so that the porous channels ran in a parasagittal (anteroposterior) direction. Muscles, fasciae, and skin incisions were repaired in layers using atraumatic resorbable sutures.

Heterotopic Implantation

Surgical procedures in the heterotopic primate model were as described previously [5, 6]. A total of 48 hydroxyapatite disks were implanted bilaterally in intramuscular pouches created by sharp and blunt dissection in the rectus abdominis, six implants per animal. Implants cut in the transversal and longitudinal planes were placed into right and left pouches, respectively. Incisions were closed in layers using atraumatic resorbable sutures.

After surgery, the animals were administered benethamine and procaine penicillins intramuscularly. Postoperative pain was controlled by intramuscular buprenorphine hydrochloride (0.3 mg). Individually housed animals were kept under daily clinical observation and fed as described previously [10].

Tissue Harvest and Histology

Anesthetized animals were killed on day 90 after the surgery with an overdose of sodium pentobarbitone. Bilateral carotid perfusion and harvest of specimens with surrounding calvaria were as described previously [9, 16]. Specimen blocks were cut into halves along the sagittal diameter of the implanted hydroxyapatite disks or untreated defects (Fig 3). Untreated defect specimens were dehydrated in ascending grades of ethanol and embedded, undecalcified, in a methyl methacrylate resin (K-Plast, Medim, Germany). Undecalcified serial sections,

7 μm thick, were cut along the sagittal plane with tungsten-carbide knives and a motor-driven microtome (Supercut 2050, Reichert-Jung, Germany). Sections were stained using the free-floating method with Goldner's trichrome for undecalcified bone. Hydroxyapatite specimens were decalcified in a formic–hydrochloric acid mixture and double-embedded in celloidin and paraffin wax. Serial sections, 7 μm thick, were stained with 0.1% toluidine blue in 30% ethanol or with the Goldner's trichrome.

Hydroxyapatite specimens, harvested from the ventral musculature, were cleaned of adherent soft tissue, fixed in 10% neutral buffered formaldehyde, and processed for decalcified histology as described above. Serial sections were cut along the longitudinal plane and stained with toluidine blue or Goldner's trichrome.

Histomorphometric Analysis

Calvarial Specimens

A calibrated Zeiss Integration Platte II with 100 lattice points was used to calculate, by point-counting technique [18], the fractional volumes (%) of each histologic component, ie, newly formed bone, soft tissues (including fibrovascular, muscle, and marrow tissue), and the implanted hydroxyapatite. Volume fraction compositions of hydroxyapatite specimens were calculated examining decalcified sections (see Fig 3). On undecalcified sections, prepared from untreated defects, bone values were computed by calculating separately its mineralized and osteoid components [9, 16]. Sections were analyzed at a magnification of 40 times, superimposing the Zeiss graticule over five sources [19], selected for histomorphometry and defined as follows: two anterior and posterior interfacial regions (AIF and PIF), two anterior and posterior internal regions (AIN and PIN), and a central region (CEN) (see Fig 3). This technique allows the histomorphometric evaluation of the distribution of bone regeneration across the untreated and treated defects [9, 16]. Each source represented a field of 7.84 mm^2. Histomorphometry was performed on one section per specimen; sections used for histomorphometry were similarly located in all specimens (see Fig 3).

Intramuscular Specimens

From each specimen harvested from the rectus abdominis, one section taken through the center was analyzed and taken to be representative of the extent of bone formation in that specimen. For the purpose of a semiquantitative analysis, the amount of induced bone was graded using values from 0 to 3 as described previously [10]: 0, none; 1, minimal amounts of induced bone; 2, moderate amounts of induced bone scattered throughout the specimen; 3, substantial bone formation within the porous spaces of the specimen.

Statistical Analysis

Data were analyzed with the Statistical Analysis System [20]. Data of the present series of 16 untreated defects in subadult baboons were compared with a previously published series of 16 calvarial defects, 25 mm in diameter, prepared in adult male baboons and harvested on day 90 [9, 17]. An F test was performed using an analysis of variance with multiple interactions. Comparison of mean values was obtained using Scheffe's multiple-comparison procedure on the dependent variables included in the analysis. A Student t test was used to compare the extent of bone formation between the heterotopic hydroxyapatite specimens. The critical level of statistical significance chosen was $p < 0.01$.

Results

Morphology of Calvarial Repair and Implant Incorporation in Subadult Baboons

Untreated defects showed limited osteogenesis, essentially confined to the margins of the severed calvariae, as described in untreated defects of adult baboons harvested on day 90 [9]. Representative histologic sections of hydroxyapatite specimens cut in the longitudinal and transversal planes are shown in Figures 4 and 5, respectively. Variable amounts of bone had formed in hydroxyapatite specimens of both geometric configurations. Histologic analysis indicated that bone first formed in direct apposition to the hydroxyapatite, and was lined by osteoblasts on its advancing surface (see Figs 4B and 5B). In hydroxyapatite cut in the transversal plane, newly formed bone was not confined to any particular region of the specimen, and the distribution of bone within the implant was not uniform. In two hydroxyapatite specimens cut in the longitudinal plane, there was total penetration of bone (see Fig 4).

Heterotopic Specimens

The amount of induced bone that formed within the porous spaces of the hydroxyapatite specimens harvested from the rectus abdominis varied from nothing to florid (Fig 6). A cellular, dense connective tissue matrix with a prominent vascular component occupied the porous spaces of the specimens. Bone formed in specimens of both geometric configuration, predominantly within the central regions of the implants.

Histomorphometry

Calvarial Specimens

Volume fractions of bone and osteoid in untreated calvarial defects of subadult baboons are summarized in Table 1. When compared with a previous series of untreated defects prepared in adult baboons, bone volume did not differ significantly between subadult and adult baboons.

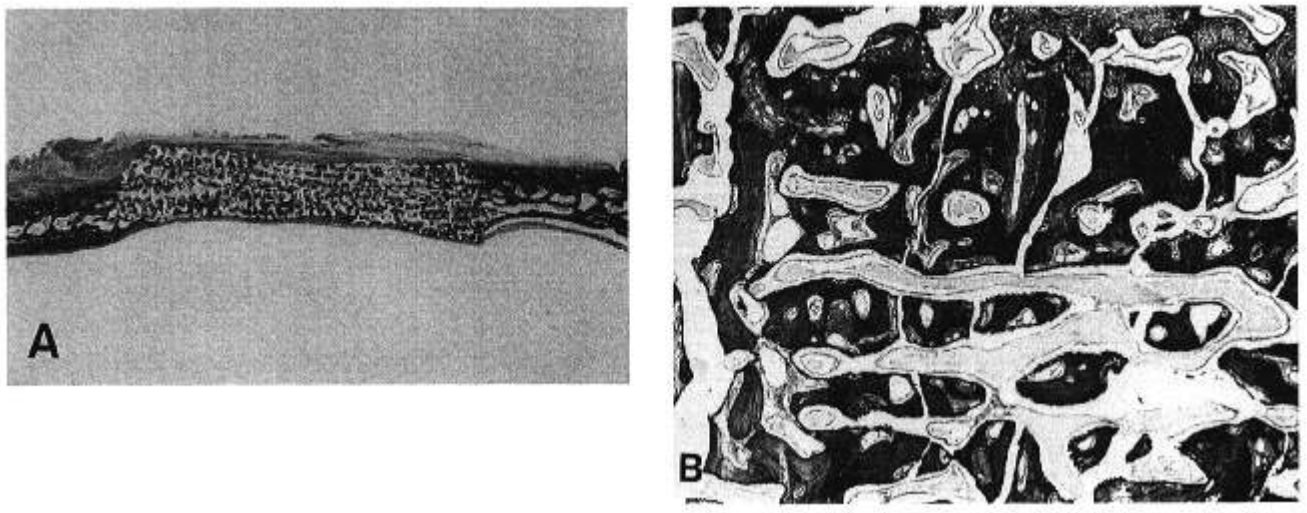

Fig 4 Photomicrographs of a hydroxyapatite specimen cut in the longitudinal plane and harvested on day 90. (A) Low-power view. Extensive bone formation and union at the calvarial interfaces. Empty white spaces represent the hydroxyapatite matrix dissolved after decalcification during histologic processing. (B) Higher magnification of previous section showing bone deposition filling the porous spaces. (Toluidine blue; original magnification: × 2.2, before 32% reduction [A], and × 15, before 28% reduction [B].)

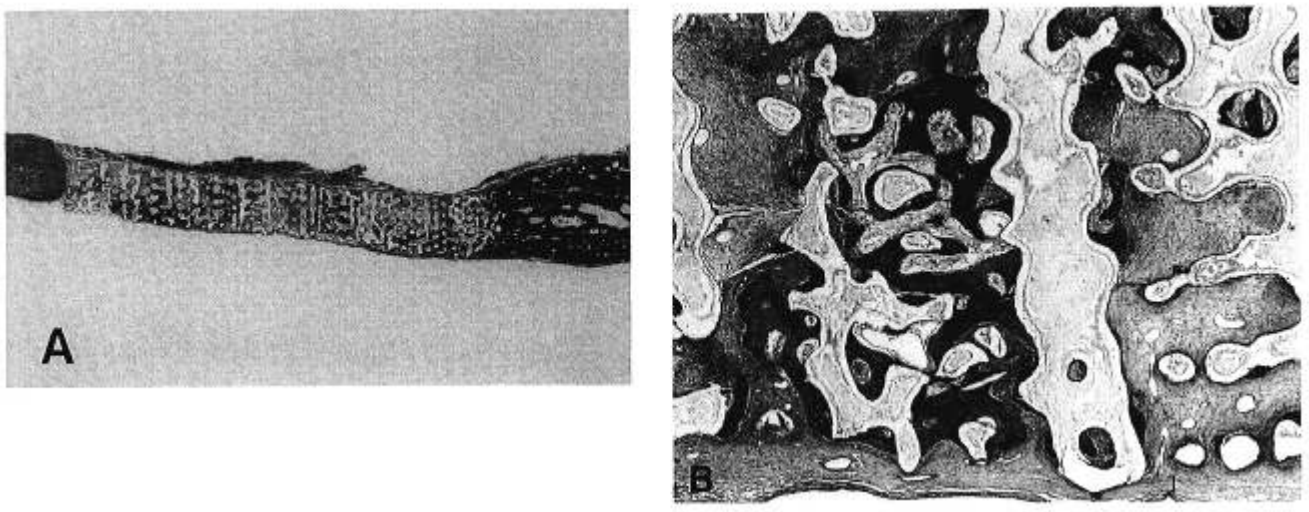

Fig 5 Hydroxyapatite specimen cut in the transversal plane. (A) Low-power view. Scattered and limited amounts of bone had formed within the porous spaces. Note the vertical orientation of the original corallite walls. (B) Higher magnification of previous section showing islands of bone formation within the porous spaces of the transversally prepared hydroxyapatite implant. (Toluidine blue; original magnification: × 2.2, before 32% reduction [A], and × 15, before 29% reduction [B].)

Table 2 illustrates the distribution of bone in untreated defects within the five sources analyzed by histomorphometry. The data show a sharp reduction of bone and osteoid volumes between the interfacial, and the internal and central regions of both subadult and adult untreated defects ($p < 0.01$; see Table 2).

Volume fraction compositions of hydroxyapatite specimens are presented in Table 3. Greater amounts of bone formed in longitudinally prepared than in transversally prepared hydroxyapatite disks ($p < 0.01$; see Table 3). Bone volume in hydroxyapatite specimens of both geometric configurations varied greatly between animals, ranging from 16.1 to 32.8%, indicating variability in animal response. The distribution of bone in hydroxyapatite specimens within the five sources analyzed by histomorphometry is presented in Table 4. In both geometric

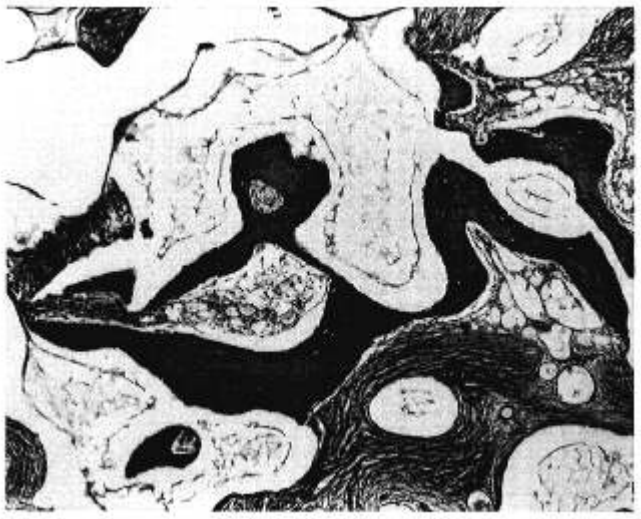

Fig 6 Photomicrograph of a heterotopic hydroxyapatite specimen (cut in the longitudinal plane) harvested from the rectus abdominis of the baboon on day 90. Bone had formed in direct contact with the hydroxyapatite (Goldner's trichrome stain; original magnification × 60, before 29% reduction).

Table 1 Volume Fraction (%) of Bone and Osteoid in 32 Untreated Calvarial Defects Harvested from Subadult and Adult Baboons on Day 90[a]

		Bone	*Osteoid*
Subadult	(n = 16)	11.8 ± 1.7	0.6 ± 0.1
Adult[b]	(n = 16)	11.7 ± 1.7	1.2 ± 0.2

Volume fraction of tissue components were calculated using a Zeiss Integration Platte II with 100 lattice points superimposed over five sources analyzed by histomorphometry as described in Materials and Methods. Bone indicates mineralized bone plus osteoid.
[a]Mean and standard error of the mean.
[b]Data from [9, 17].

Table 2 Distribution of Bone and Osteoid (%) Within Histomorphometric Sources in 32 Untreated Calvarial Defects Harvested from Subadult and Adult Baboons on Day 90[a]

	Subadult		*Adult*[b]	
Source	*Bone*	*Osteoid*	*Bone*	*Osteoid*
	$p < 0.01$	$p < 0.01$	$p < 0.01$	$p < 0.01$
AIF	25.3 ± 3.8	1.1 ± 0.3	29.3 ± 4.1	2.8 ± 0.6
AIN	3.4 ± 1.8	0.5 ± 0.3	5.9 ± 2.1	0.8 ± 0.4
CEN	0.9 ± 0.9	0.0	2.9 ± 1.8	0.2 ± 0.1
PIN	2.7 ± 1.6	0.1 ± 0.1	3.4 ± 1.7	0.4 ± 0.3
PIF	26.8 ± 3.0	1.2 ± 0.3	16.9 ± 3.6	1.9 ± 0.6

p values indicate level of significance between sources. Sources were as follows: AIF = anterior interfacial; AIN = anterior internal; CEN = central; PIN = posterior internal; PIF = posterior interfacial.
[a]Mean and standard error of the mean.
[b]Data from [9, 17].

Table 3 Volume Fraction Composition (%) of 16 Hydroxyapatite Specimens Harvested from Eight Subadult Baboons on Day 90[a]

Treatment	*Bone*	*Soft Tissue*	*Hydroxyapatite*
Hydroxyapatite prepared longitudinally (n = 8)	29.1 ± 2.6[b]	39.0 ± 2.6[b]	31.9 ± 1.1
Hydroxyapatite prepared transversally (n = 8)	21.0 ± 2.1	45.0 ± 2.2	32.6 ± 1.2

[a]Mean and standard error of the mean.
[b]$p < 0.01$ versus transversally prepared hydroxyapatite specimens.

configurations, on average, greater amounts of bone formed at the interfacial and internal regions when compared with the central regions. This pattern of bone distribution was most obvious in transversally prepared disks where bone volume between interfacial and central regions differed significantly ($p < 0.01$; see Table 4). It is noteworthy that, on average, longitudinally and transversally prepared disks did not differ from each other with regard to the volume of hydroxyapatite, as measured by histomorphometry on day 90 after implantation.

Heterotopic Hydroxyapatite Specimens

Results of the semiquantitative analysis showed the means of induced bone in longitudinally and transversally prepared disks to be almost identical, with no significant difference between the two geometric configurations (not shown).

Discussion

Porous hydroxyapatites obtained by hydrothermal conversion of the calcium carbonate exoskeleton of corals have been the subject of extensive investigation in several animal models for potential craniofacial therapeutic applications [4, 9, 14, 21, 22]. Although emphasis has focused primarily on surface characteristics and pore size as a function of osteoconductivity, the importance of implant geometry has been comparatively neglected. The importance of the geometry of the substratum on cell differentiation has been demonstrated previously [23, 24]. Using demineralized bone and dentine matrices as inductive substrata, it was shown that the geometry of the implanted matrix influenced profoundly the expression of the chondro-osteogenic phenotype in vivo [25, 26]. More

Table 4 Distribution of Bone and Hydroxyapatite Within Sources in 16 Hydroxyapatite Specimens Harvested from Eight Subadult Baboons on Day 90[a]

	Hydroxyapatite Prepared Longitudinally (n = 8)		*Hydroxyapatite Prepared Transversally (n = 8)*	
Source	*Bone*	*Hydroxyapatite*	*Bone*	*Hydroxyapatite*
	NS		$p < 0.01$	
AIF	38.4 ± 4.0	26.8 ± 2.7	33.5 ± 2.9	29.8 ± 2.7
AIN	26.3 ± 3.9	33.3 ± 1.9	21.0 ± 3.8	35.0 ± 2.6
CEN	19.5 ± 4.1	36.3 ± 2.6	12.0 ± 3.1	32.6 ± 2.4
PIN	28.0 ± 4.2	31.8 ± 2.6	16.6 ± 3.4	35.6 ± 2.9
PIF	33.3 ± 3.8	29.8 ± 2.8	24.8 ± 3.4	30.1 ± 2.8

p values indicate level of significance between sources. NS = nonsignificant.
[a]Mean and standard error of the mean.
AIF = anterior interfacial; AIN = anterior internal; CEN = central; PIN = posterior internal; PIF = posterior interfacial.

recently, the critical role of implant geometry was demonstrated by experimental studies on heterotopic osteogenesis in porous hydroxyapatites in both rodents [8] and primates [7].

In the present experiment, more bone was generated in longitudinally prepared disks when compared with transversally prepared hydroxyapatite disks implanted in calvarial defects of subadult baboons. The orientation of the porous configuration of the longitudinally prepared disks might have promoted superior osteoconductivity, possibly as a function of faster fibrovascular tissue ingrowth. Angiogenesis is a prerequisite for osteogenesis [27], and a defined orientation of the porous spaces may be more conducive to rapid vascular invasion.

Comparatively limited information exists on the importance of geometry on bone formation of biomaterials other than coral-derived porous hydroxyapatites. Omnidirectional tricalcium phosphate disks inserted into 15-mm-diameter calvarial defects of rabbits were more effective than unidirectional porous implants when evaluated on histological criteria [28]. More recently, it was shown that the surface topography of macromachined implants enhanced mineralized tissue formation in vitro and influenced bone formation in vivo [29, 30]. Other in vitro experiments have indicated that the orientation of gingival fibroblasts is influenced by the surface geometry of the substratum [31].

Although the geometric configurations did not affect the extent of bone formation in the heterotopic specimens, the differentiation of bone in hydroxyapatite disks implanted in the rectus abdominis is noteworthy. This confirms and extends previous results on identical, albeit of smaller dimension, porous hydroxyapatite implanted in heterotopic sites of the baboon [5, 6]. Because adsorption of mammalian BMPs on hydroxyapatite gels is a fundamental step for their purification [32, 33], heterotopic osteogenesis in porous hydroxyapatite in the baboon may be the result of adsorption of endogenously produced BMPs and induction of bone as a secondary response [5, 6]. In these studies we have reported extensive bone differentiation in rods of porous hydroxyapatite of 7-mm diameter when implanted intramuscularly in baboons. In the present series, using disks of 25 mm in diameter, bone formation was discrete in some specimens yet absent from others. It is likely that the dimension of the implants is of importance in determining the extent of bone formation in larger specimens when evaluated on day 90. The increase in implant size may affect the rate and extent of centripetal fibrovascular tissue invasion, resulting in delayed osteogenesis.

The finding that osteogenesis in untreated defects of subadult baboons is comparable with the extent of bone formation in untreated defects of adult baboons is noteworthy. This combined series of 32 calvarial defects in baboons is unique, and warranted a comparative analysis between subadult and adult calvariae. Experimental evidence in rats [34] and baboons [35] has indicated that limited osteogenesis in calvarial defects may be related to fusion of the pericranium with the dura, after the penetration of the temporalis muscle within the defects. Thus, the most likely reason for otherwise nonhealing calvarial defects is intrusion of cell populations migrating from nonosteogenic sources into the defects [34, 36], rather than an intrinsic limited regenerative capacity of both subadult and adult animals.

In conclusion, the results of this study in primates indicate that the geometric configuration of porous hydroxyapatite influences the extent of bone growth and osteogenesis in orthotopic calvarial sites of subadult baboons, and that porous hydroxyapatite disks are able to induce bone differentiation when implanted in intramuscular sites. The control of implant geometry and the

concept of intrinsic osteoinductivity of certain porous biomaterials may have important implications for craniofacial skeletal repair.

Supported by grants from the South African Medical Research Council and the University of the Witwatersrand, Johannesburg.

We thank B. van den Heever for invaluable help with histology, Dr T. Moehl and M. Hendrikse for surgical assistance and monitoring of primates, and Dr E. C. Shors and Interpore International, California, for the preparation of the hydroxyapatite implants.

References

1. Jarcho M. Calcium phosphate ceramics as hard tissue prosthetics. Clin Orthop 1981;157:259-278
2. Hench LL, Wilson J. Surface-active biomaterials. Science 1984; 226:630-636
3. Ripamonti U, Reddi AH. Bone morphogenetic proteins: applications in plastic and reconstructive surgery. Adv Plast Reconstr Surg 1995;11:47-73
4. Holmes RE, Hagler HK. Porous hydroxyapatite as a bone graft substitute in cranial reconstruction: a histometric study. Plast Reconstr Surg 1988;81:662-671
5. Ripamonti U. The morphogenesis of bone in replicas of porous hydroxyapatite obtained from conversion of calcium carbonate exoskeletons of coral. J Bone Joint Surg [Am] 1991;73:692-703
6. Ripamonti U, van den Heever B, van Wyk J. Expression of the osteogenic phenotype in porous hydroxyapatite implanted extraskeletally in baboons. Matrix 1993;13:491-502
7. van Eeden S, Ripamonti U. Bone differentiation in porous hydroxyapatite in baboons is regulated by the geometry of the substratum: implications for reconstructive craniofacial surgery. Plast Reconstr Surg 1994;93:959-966
8. Ripamonti U, Ma S, Reddi AH. The critical role of geometry of porous hydroxyapatite delivery system in induction of bone by osteogenin, a bone morphogenetic protein. Matrix 1992;12:202-212
9. Ripamonti U. Calvarial reconstruction in baboons with porous hydroxyapatite. J Craniofac Surg 1992;3:149-159
10. Ripamonti U. Bone induction in nonhuman primates. An experimental study on the baboon. Clin Orthop 1991;269:284-293
11. Napier JR, Napier PH. The natural history of primates. Ipswich: Cambridge University Press, 1985
12. Wells JW. Scleractinia. In: Moore RC, ed. Treatise on invertebrate paleontology. Kansas City: University of Kansas Press, 1956:328-444
13. Roy DM, Linnehan SK. Hydroxyapatite formed from coral skeletal carbonate by hydrothermal exchange. Nature 1974;247:220-222
14. White EW, Weber JN, Roy DM, Owen EL. Replamineform porous biomaterials for hard tissue implant applications. J Biomed Mater Res 1975;9:23-27
15. Holmes RE, Bucholz RW, Mooney V. Porous hydroxyapatite as a bone graft substitute in metaphyseal defects. A histometric study. J Bone Joint Surg [Am] 1986;68:904-911
16. Ripamonti U, Ma S, van den Heever B, Reddi AH. Osteogenin, a bone morphogenetic protein, adsorbed on porous hydroxyapatite substrata, induces rapid bone differentiation in calvarial defects of adult primates. Plast Reconstr Surg 1992;90:382-393
17. Ripamonti U, Ma S, Cunningham N, et al. Reconstruction of the bone-bone marrow organ by osteogenin, a bone morphogenetic protein, and demineralized bone matrix in calvarial defects of adult primates. Plast Reconstr Surg 1993;91:27-36
18. Parfitt AM. Stereologic basis of bone histomorphometry: theory of quantitative microscopy and reconstruction of the third dimension. In: Recker RR, ed. Bone histomorphometry: technique and interpretation. Boca Raton: CRC Press, 1983:53-87
19. Parfitt AM, Drezner MR, Glorieux FH, et al. Bone histomorphometry: standardization of nomenclature, symbols and units (report of the ASBMR Histomorphometry Nomenclature Committee). J Bone Miner Res 1987;2:595-601
20. Statistical Analysis System. SAS/STAT user's guide: version 6. 4th ed. Cary, NC: SAS Institute, 1989:891-996
21. Holmes RE. Bone regeneration within a coralline hydroxyapatite implant. Plast Reconstr Surg 1979;63:626-633
22. Holmes RE, Hagler HK. Porous hydroxyapatite as a bone graft substitute in maxillary augmentation. A histometric study. J Craniomaxillofac Surg 1988;16:199-205
23. Reddi AH. Bone matrix in the solid state: geometric influence on differentiation of fibroblasts. Adv Biol Med Phys 1974;15:1-18
24. Folkman J, Greenspan HP. Influence of geometry on the control of cell growth. Biochem Biophys Acta 1975;417:211-236
25. Reddi AH, Huggins CB. Influence of geometry of transplanted tooth and bone on transformation of fibroblasts. Proc Soc Exp Biol Med 1973;143:634-637
26. Sampath TK, Reddi AH. Importance of geometry of the extracellular matrix in endochondral bone differentiation. J Cell Biol 1984;98:2192-2197
27. Trueta J. The role of the vessels in osteogenesis. J Bone Joint Surg [Br] 1963;45:402-418
28. Hollinger JO, Schmitz JP, Mixgala JW, Hassler C. An evaluation of two configurations of tricalcium phosphate for treating craniotomies. J Biomed Mater Res 1989;23:17-29
29. Brunette DM, Ratkay J, Chehroudi B. The behaviour of osteoblasts on macromachined surfaces. In: Davies JE, ed. The bone-biomaterial interface. Toronto: University of Toronto Press, 1991: 170-180
30. Chehroudi B, Ratkay J, Brunette DM. The role of implant surface geometry on mineralization in vivo and in vitro; a transmission and scanning electron microscope study. Cells Materials 1992;2: 89-104
31. Inoue T, Cox JE, Pilliar RM, Melcher AH. Effect of the surface geometry of smooth and porous-coated titanium alloy on the orientation of fibroblasts *in vitro*. J Biomed Mater Res 1987;21: 107-126
32. Sampath TK, Muthukumaran N, Reddi AH. Isolation of osteogenin, an extracellular matrix-associated bone inductive protein, by heparin-affinity chromatography. Proc Natl Acad Sci USA 1987;84:7109-7113
33. Luyten FP, Cunningham N, Ma S, et al. Purification and partial amino acid sequence of osteogenin, a protein initiating bone differentiation. J Biol Chem 1989;264:13377-13380
34. Dahlin C, Alberius P, Linde A. Osteopromotion for cranioplasty: an experimental study in rats using a membrane technique. J Neurosurg 1991;47:487-491
35. Petit J-C, Ripamonti U. Tissue segregation enhances calvarial osteogenesis in adult primates. J Craniofac Surg 1994;5:34-43
36. Dahlin C, Linde A, Gottlow J, Nyman S. Healing of bone defects by guided tissue regeneration. Plast Reconstr Surg 1988;81:672-676